Highly Viscous Accretion Disks with Advection

I.V.Artemova[1],
Theoretical Astrophysics Center, Juliane Maries Vej 30, DK-2100, Copenhagen Ø, Denmark

G.S. Bisnovatyi-Kogan[2],
Space Research Institute, Profsoyuznaya 84/32, 117810 Moscow, Russia

G. Björnsson[3],
Science Institute, Dunhagi 3, University of Iceland, IS-107 Reykjavik, Iceland

I.D. Novikov[4]

Theoretical Astrophysics Center, Juliane Maries Vej 30, DK-2100, Copenhagen Ø, Denmark

University Observatory, Juliane Maries Vej 30, DK-2100, Copenhagen Ø, Denmark

NORDITA, Blegdamsvej 17, DK-2100 Copenhagen Ø, Denmark

Astro Space Center of P.N. Lebedev Physical Institute, Profsoyuznaya 84/32, 117810
Moscow, Russia

Received ______________________; accepted ______________________

[1]e-mail:julia@nordita.dk

[2]e-mail:Gkogan@mx.iki.rssi.ru

[3]e-mail:gulli@raunvis.hi.is

[4]e-mail:novikov@nordita.dk

ABSTRACT

We consider the effects of advection and radial gradients of pressure and radial drift velocity on the structure of optically thick accretion disks. We concentrate our efforts on highly viscous disks, $\alpha = 1.0$, with large accretion rates. Contrary to disk models neglecting advection, we find that continuous solutions extending from the outer disk regions to the inner edge exist for all accretion rates we have considered. We show that the sonic point moves outward with increasing accretion rate, and that in the innermost disk region advection acts as a heating process that may even dominate over dissipative heating. Despite the importance of advection on it's structure, the disk remains geometrically thin.

Subject headings: accretion, accretion disks - black hole physics

1. Introduction

The "standard accretion disk model" of Shakura (1972) and Shakura & Sunyaev (1973), that has been widely used to model accretion flows around black holes, is based on a number of simplifying assumptions. In particular, the flow is assumed to be geometrically thin and with a Keplerian angular velocity distribution. This assumption allows gradient terms in the differential equations describing the flow to be neglected, reducing them to a set of algebraic equations, and thereby fixes the angular momentum distribution of the flow. For low accretion rates, $\dot{M}$, this assumption is generally considered to be reasonable.

Since the end of the seventies, however, it has been realized that for high accretion rates, advection of energy with the flow can crucially modify the properties of the innermost parts of accretion disks around black holes. A deviation from a Keplerian rotation may result.

Initial attempts to solve the more general disk problem only included advection of energy and the radial gradient of pressure in models with small values of the viscosity parameter, $\alpha = 10^{-3}$ (Paczyński & Bisnovatyi-Kogan 1981), and it was shown that including radial velocity in the radial momentum equation would not change principally the results for such a small α (Muchotrzeb & Paczyński 1982). Liang & Thomson (1980) emphasised the importance of the transonic nature of the radial drift velocity, and the influence of viscosity on the transonic accretion disk solutions was noted by Muchotrzeb (1983), who claimed that such solutions only existed for viscosity parameters smaller than $\alpha_* \simeq 0.02 - 0.05$. Matsumoto et al. (1984), then showed that solutions with $\alpha > \alpha_*$ do in fact exist, but the nature of the singular point, where the radial velocity equals the sound velocity, is changing from a saddle to a nodal type and the position of this point is shifted substantially outwards in the disk. Matsumoto et al. (1984) also demonstrated the non-uniqueness of the solutions with a nodal type critical point for given Keplerian

boundary conditions at the outer boundary of the disk (see also Muchotrzeb-Czerny 1986). Extensive investigation of accretion disk models with advection for a wide range of the disk parameters, $\dot{M}$ and α, was conducted by Abramowicz et al. (1988), with special emphasis on low α. Misra & Melia (1996) considered optically thin two-temperature disk models and treated advection in the framework of the Keplerian disk model, but fixed the proton temperature somewhat arbitrarily at the outer boundary. Chakrabarti (1996) solved the advection problem containing shock waves near the innermost disk region, considering accretion through saddle points. Numerical solutions of accretion disks with advection have been obtained by Chen and Taam (1993) for the optically thick case with $\alpha = 0.1$, and by Chen et al. (1996), for the optically thin case (see also Narayan 1996). A simplified account of advection has recently been attempted, either treating it like an additional algebraic term assuming a constant radial gradient of entropy (Abramowicz et al. 1995; Chen et al. 1995; Chen 1995), or using the condition of self-similarity (Narayan & Yi 1994).

Over the last few years it has become clear, that neglecting the advective heat transport at high $\dot{M}$ leads to qualitatively wrong conclusions about the topology of the family of solutions of the disk structure equations (see for example Abramowicz et al. 1995; Chen et al. 1995; Artemova et al. 1996). The disk structure equations without advection give rise two branches of solutions: optically thick and optically thin, which do not intersect if $\dot{M} < \dot{M}_b \approx (0.6 - 0.9)\dot{M}_{\rm Edd}$ for $\alpha = 1$ and $M_{BH} = 10^8 M_\odot$, where $\dot{M}_{\rm Edd}$ is the Eddington accretion rate (Artemova et al. 1996). For larger accretion rates there are no solutions of these equations extending continuously from large to small radii, and with Keplerian boundary conditions at the outer boundary of the disk (see also Liang & Wandel 1991; Wandel & Liang 1991; Luo & Liang 1994). It was argued by Artemova et al. (1996), that for accretion rates larger than $\dot{M}_b$, advection becomes critically important and would allow solutions extending all the way to the inner disk edge also to exist for $\dot{M} > \dot{M}_b$.

The goal of the present paper is to construct explicitly accretion disk models for high $\dot{M}$ and large α taking advective heat transport self-consistently into account. We also include radial gradients of pressure and radial drift velocity and we allow for the non-Keplerian character of the circular velocity. Furthermore, we use the geometrically thin disk approximation because, as will be seen in our solutions, the relative thickness of the disk is substantially less than unity. We show that solutions extending from large radii to the inner edge of the disk can be constructed even for accretion rates considerably larger than $\dot{M}_b$. We find that advection is very important in the innermost disk region, although the flow does not deviate strongly from Keplerian down to the region where the radial inflow velocity approaches the local sound speed.

In §2 we introduce our model and describe our solution methods, while in §3 we discuss our results.

2. The Model and the Method of Solution

In this paper we will only consider optically thick solutions to the disk equations. When advective cooling is important we assume that it can be sufficiently well modelled by adding it self-consistently to other cooling mechanisms in a geometrically thin disk.

We use from now on geometric units with $G = 1$, $c = 1$, use r as the radial coordinate scaled to $r_g = M$, and scale all velocities to c. We work with the pseudo-Newtonian potential proposed by Paczyński and Wiita (1980), $\Phi = -M/(r-2)$, that provides an accurate, yet simple approximation to the Schwarzschild geometry. We normalise the accretion rate as $\dot{m} = \dot{M}/\dot{M}_{\rm Edd}$, where $\dot{M}_{\rm Edd} = L_{\rm Edd} = 4\pi M m_p/\sigma_T$, in our units.

We use the same equations and ingredients in our models as in Artemova et al. (1996), except for changes required by the Paczyński-Wiita potential and the differential terms

in the energy equation and the radial momentum equation. The following equations are therefore modified:

1. Conservation of angular momentum for a steady-state accretion in the α-disk model, is written as

$$\dot{m}\,(r_g\Omega)\,\frac{3}{2}\left|\frac{d\ln\Omega}{d\ln r}\right|^{-1} f = \left(\frac{\sigma_{\rm T}}{m_{\rm p}}\right) h\alpha P, \tag{1}$$

where, Ω, is the angular velocity, the factor $f = 1 - l_{\rm in}/l$, where, $l = r^2\Omega$, is the specific angular momentum and $l_{\rm in}$ is the value of l lost from the disk at the innermost edge and swallowed by the black hole. The half thickness of the disk is denoted by h, and P is the total pressure in the equatorial plane of the disk.

2. The energy equation has the form

$$Q_+ = Q_{\rm adv} + Q_{\rm loc}, \tag{2}$$

where $Q_{\rm loc}$ is in general the total rate of all local cooling processes (see Artemova et al. 1996), and the viscous heating rate per unit area, Q_+, is given by the formula (see e.g. Bisnovatyi-Kogan 1989; Frank, King & Raine, 1992)

$$\left(\frac{r_g\sigma_{\rm T}}{3m_{\rm p}}\right) Q_+ = \dot{m}\,(r_g\Omega)^2\,\frac{2}{3}\left|\frac{d\ln\Omega}{d\ln r}\right| f. \tag{3}$$

The advective cooling rate can be written in the form (see e.g. Chen & Taam 1993):

$$Q_{\rm adv} = -\frac{\dot{M}}{2\pi r}T\frac{dS}{dr} = -\frac{\dot{M}}{2\pi r}\left[\frac{dE}{dr} + P\frac{dv}{dr}\right], \tag{4}$$

where T is the temperature and S is the specific entropy. Here, E is the energy per unit mass of the gas and $v = 1/\rho$, where ρ is the matter density. With $Q_{\rm adv}$ of the form given in equation (4), the energy balance becomes a differential equation.

3. The momentum equation in the radial direction takes into account pressure and radial velocity gradients and is written in the form:

$$\frac{1}{\rho}\frac{dP}{dr} = (\Omega^2 - \Omega_{\rm K}^2)r - v_r\frac{dv_r}{dr}, \tag{5}$$

where, $\Omega_{\rm K} = \sqrt{(\partial\Phi/\partial r)/r}$, is the Keplerian angular velocity in the Paczyński-Wiita potential and v_r is the radial drift velocity. Neglecting the gradient terms in equation (5), as is done in the standard model, fixes $\Omega = \Omega_{\rm K}$.

From equation (5) and mass conservation one gets:

$$\frac{d\ln v_r}{d\ln r} = \frac{a_s^2(1 + (d\ln h)/(d\ln r)) + r^2(\Omega^2 - \Omega_{\rm K}^2)}{v_r^2 - a_s^2}, \tag{6}$$

where a_s is defined as (Muchotrzeb & Paczyński 1981):

$$a_s^2 = \left(\frac{dP}{dr}\right)\left(\frac{d\rho}{dr}\right)^{-1} \tag{7}$$

Note, that a_s is *not* a physical sound velocity but rather a formal quantity. The vanishing of both the numerator and the denominator in equation (6) at the same value of r, the "sonic point", provides the regularity condition required for a "transonic solution" of the flow structure.

To solve the differential equations (2) and (5) we adopt the following boundary conditions: At large radii, $r \gg 100$, the solution must coincide with the standard Keplerian disk solution obtained neglecting advection. In addition, the parameter $l_{\rm in}$ in equations (1) and (3), is an eigenvalue of the problem which is adjusted in such a way that the solution satisfies the regularity condition at the "sonic point".

We solved this system of equations numerically by the method of subsequent iterations with fixed $\dot{m}$ and α. Starting from the "standard disk" solution as the initial trial solution with a specific value of $l_{\rm in}$ in the function, $f = 1 - l_{\rm in}/l$, we then varied $l_{\rm in}$ to obtain a self-consistent solution. Typically the method converges to a solution after three to four iterations.

In practice, we varied $l_{\rm in}$ in some interval and determined the positions of the points r_N and r_D where the numerator and the denominator of equation (6) vanish, respectively.

We then considered the dependence of the difference $(r_D - r_N)$ on $l_{\rm in}$ and determined $l_{\rm in}$ for which the difference $(r_D - r_N)$ is equal to zero. The corresponding $l_{\rm in}$ is an eigenvalue of the problem. Examples of the dependences $(r_D - r_N)$ on $l_{\rm in}$ are given in Figure 1 for $\dot{m} = 10.0$ (accretion rate less than $\dot{m}_b$), and $\dot{m} = 28.0$ (accretion rate substantially greater than $\dot{m}_b$).

For $\dot{m} > \dot{m}_b$, our method is very sensitive to the choice of the initial trial solution in the innermost disk region. Using a "standard disk" solution down to $r = 6$ is not possible, as for these large values of $\dot{m}$ there is no solution around $r \approx 13$, and the method cannot bridge that gap to find a "transonic" solution. For our initial trial solution, we therefore chose a value of $l_{\rm in}$ that allowed us to generate the trial solution down to small radii, and then iterated as described above.

As is seen in Fig. 1, there are three values of $l_{\rm in}$ for each $\dot{m}$, where $(r_D - r_N) = 0$, and some range of $l_{\rm in}$ where $(r_D - r_N)$ is very close to zero. Most likely that range corresponds to the nodal type of a sonic point at large α, as obtained by Matsumoto et al. (1984) and others under some simplifications. In this case the condition of regularity at the sonic point does not specify $l_{\rm in}$ uniquely. From our numerical method we are unable to determine if any $l_{\rm in}$ in the range of $l_{\rm in}$'s, where $r_D - r_N$ is close to zero, provides an acceptable solution. Complete analysis of the character of the critical points needs a different approach and will be performed elsewhere (but see next section).

Our method allows us to construct a self-consistent solution to the system of equations from very large radii, $r > 100$, and down to the innermost regions of the disk. The solution passes through a "sonic point" and continues closer towards the black hole. But, we cannot construct the parts of the solutions in the very vicinity of the black hole where the angular velocity is very far from Keplerian and l is almost constant. However, in all cases do we extend the solutions down to the value of r at which v_r becomes equal to the local adiabatic sound velocity. These radii are in general closer to the black hole than the location of the

“sonic point”.

3. Results and Discussion

In Table 1 we summarise the parameters of the models for which $r_D - r_N = 0$, according to our computations. For each fixed $\dot{m}$, the properties of the two (or three) self-consistent solutions are similar and differ only quantitatively. In all cases discussed below do we take $M_{BH} = 10^8 M_\odot$ and $\alpha = 1$.

We will now compare the solutions with and without advection. In the “standard model”, for accretion rates $\dot{m} < \dot{m}_b = 14.315$, there always exist solutions that extend continuously from large to small radii. When $\dot{m} > \dot{m}_b = 14.315$ there are no solutions in a range of radii around $r \approx 13$, and therefore no continuous solutions extending from large radii to the innermost disk edge (see detailed discussion by Artemova et al. 1996, where however, the Newtonian potential was used, resulting in $\dot{m}_b = 9.4$).

In Figure 2a we plot the disk surface density $\Sigma = 2\rho h$, in an optically thick disk as a function of radius, r, in a model with $\dot{m} = 10$. The lowest curve is the solution of the standard model, the upper ones are solutions number 2 and 3 in Table 1. Note that the solutions including advection all terminate at radii considerably greater than $r = 6$ (inner edge of the disk in the standard model).

In Fig. 2b we plot similarly the solutions for $\dot{m} = 15$. In the standard model, no solution exists in the region around $r \approx 13$, but when advection is included, the structure of the solutions is completely different. Models 6 and 7 in Table 1 are shown.

For $\dot{m} < 13$, including the gradient terms gives rather small corrections to the standard disk model, see Figure 2a. When $\dot{m} > 13$ advection becomes essential and for $\dot{m} > \dot{m}_b$ it changes the picture qualitatively. When $\dot{m} > \dot{m}_b$ solutions do exist extending continuously

from large radii to the innermost disk region where the solution passes through a "sonic point" (compare Figs 2a and 2b, see also Fig 4b below). As mentioned above (see the end of Section 2), we can extend our models only down to the region where the radial velocity becomes equal to the local adiabatic sound velocity. We are unable to calculate the properties of the flow for smaller radii. Only more detailed analysis of this region (using other methods) allows one to determine the smoothness of the flow down to the event horizon of a black hole or verify the presence or absence of shocks in the region.

In Figure 3 we plot a family of optically thick solutions for different $\dot{m}$, clearly demonstrating that the solutions to the complete system of disk structure equations including advection and radial gradients have quite different properties at high $\dot{m}$ compared to the solutions of the standard disk model.

In Figure 4a we plot $Q_{\rm adv}/Q_+$ as a function of radius for $\dot{m} = 10$ and $\dot{m} = 28$, that bracket the cases we have studied. Outside the radius where the entropy gradient is zero (and therefore $Q_{\rm adv} = 0$, recall eq. [4]), advection provides an additional cooling, that is however, never substantial in our models. On the other hand, inside that radius, advection acts as a heating process that easily dominates over the dissipation rate that decreases rapidly near the inner edge of the disk (as $f \to 0$, see eq. [3]). Panels 4b and 4c show the corresponding Mach numbers and h/r-ratio, respectively. Note that although the flow becomes transonic in the inner region, the disk can still be considered geometrically thin.

In our calculations, the non-uniqueness of solutions at large $\alpha > \alpha_*$, passing through the critical point (Matsumoto et al. 1984; Muchotrzeb-Czerny 1986), is preserved. It is sill not clear, if this non-uniqueness is a realistic physical fact which explanation may be highly problematic (see for example Kato et al. 1988, where the authors argue that the fact that the transonic point is a nodal type critical point is equivalent to an instability condition), or is a result of restrictive precision of our numerical solutions. Two possible approaches

to clarify the situation can be suggested. In the first one, we could obtain an asymptotic solution of the disk equations near the gravitational radius and try to match it with the numerical solution going from the nodal point towards the inside. The second approach could be finding stationary solution by solving equations of non-stationary accretion with the appropriate boundary conditions. Both approaches need substantial numerical work, that we plan to undertake in the future.

We would like to thank M. Abramowicz for very constructive and friendly criticism of the early version of the paper and helpful suggestions. We gratitude A. Dolgov and A. Doroshkevich for discussion and E. Kotok for help. This paper was supported in part by the Danish Natural Science Research Council through grant 11-9640-1, in part by Danmarks Grundforskningsfond through its support for the establishment of the Theoretical Astrophysical Center. G.B. thanks NORDITA and TAC for partial support and hospitality, and acknowledges partial support form the Research Fund of the University of Iceland. G.B.-K. thanks TAC and Astronomy Units of Queen Mary and Westfield College for partial support and hospitality during the initial stages of this work. This work was partially supported by the Nordic Project on Non-linear Phenomena in Accretion Disks around Black Holes.

REFERENCES

Abramowicz, M.A., Czerny, B., Lasota, J.-P. & Szuszkiewicz, E. 1988, ApJ, 332, 646

Abramowicz, M.A., Chen, X., Kato, S., Lasota, J.-P. & Regev, O. 1995, ApJ, 438, L37

Artemova, I.V., Björnsson, G., Bisnovatyi-Kogan, G.S. & Novikov, I.D. 1996, ApJ, 456, 119

Chakrabarti, S.K. 1996, ApJ, 464, 664

Chen, X., Abramowicz, M.A., Lasota, J.-P., Narayan, R. & Yi, I. 1995, ApJ, 443, L61

Chen, X. & Taam, R.E. 1993, ApJ, 412, 254

Chen, X. 1995, MNRAS, 275, 641

Chen, X., Abramowicz, M.A., Lasota, J.-P., 1996, ApJ, submitted.

Bisnovatyi-Kogan, G.S., 1989, *"Physical Problems of the Theory of Stellar Evolution"*, Nauka, Moscow, (*in Russian*)

Frank, J., King, A. & Raine, D. 1992, *"Accretion Power in Astrophysics"*, Cambridge University Press, Cambridge, UK

Kato, S., Honma, F. & Matsumoto, R. 1988, PASJ, 40, 709

Liang, E.P. & Thompson, K.A. 1980, ApJ, 240, 271

Liang, E.P. & Wandel, A. 1991, ApJ, 376, 746

Luo, C. & Liang, E.P. 1994, MNRAS, 266, 386

Matsumoto, R., Kato, S., Fukue, J. & Okazaki, A.T., 1984, PASJ, 36, 71

Misra, R. & Melia, F. 1996, ApJ, 465, 869

Muchotrzeb, B. 1983, Acta Astron., 33, 79

Muchotrzeb-Czerny, B. 1986, Acta Astron.,36, 1

Muchotrzeb, B. & Paczyński, B. 1982, Acta Astron.,32, 1

Narayan, R. & Yi, I. 1994, ApJ, 428, L13

Narayan, R. 1996, in *"Basic Physics of Accretion Discs"*, ed. S. Kato et al., (New York : Gordon and Breach) in press

Paczyński, B. & Bisnovatyi-Kogan, G.S. 1981, Acta Astron., 31, 3

Paczyński, B. & Wiita, P.J. 1980, A&A, 88, 23

Shakura, N.I. & Sunyaev, R.A. 1973, A&A, 24, 337

Shakura, N.I. & Sunyaev, R.A. 1976, MNRAS, 175, 613

Wandel, A. & Liang, E.P. 1991, ApJ, 380, 84

This manuscript was prepared with the AAS LaTeX macros v4.0.

FIGURE CAPTIONS

Fig. 1. Difference $(r_D - r_N)$ as a function of $l_{\rm in}$, the angular momentum swallowed by the black hole. The 3 zero-points correspond to the solutions satisfying the regularity condition (eq. [6]), and the corresponding $l_{\rm in}$ are the eigenvalues of the problem. (a) Accretion rate of $\dot{m} = 10$ and (b) $\dot{m} = 28$.

Fig. 2. Disk surface density, $\Sigma = 2\rho h$, as a function of radius, comparing solutions with and without advection. (a) Here, $\dot{m} = 10$. The solid curve is the standard solution without advection. The dotted curve has $l_{\rm in} = 3.782$ and the dashed curve has $l_{\rm in} = 4.025$ (models 2 and 3 in Table 1). (b) The case $\dot{m} = 15$. Again the solid curve is the standard model without advection. Notice the 'no solution' region around $r \approx 13$. The dotted curve has $l_{\rm in} = 4.125$ and the dashed curve has $l_{\rm in} = 4.513$ (models 6 and 7 in Table 1).

Fig. 3. Surface density, Σ, as a function of radius for $\alpha = 1.0$ and different accretion rates. The solid curve is for $\dot{m} = 1.0$, the long dashed, short dashed, dotted and dash-dotted curves have $\dot{m} = 10, 15, 19$ and 28, respectively (models 2, 6, 10 and 13, respectively).

Fig. 4. Comparing the solutions for $\dot{m} = 10$ (dashed curve) and $\dot{m} = 28$ (solid curve) with $\alpha = 1.0$, that bracket most of the cases we have studied. (a) Ratio of advective rate (eq. [4]) to viscous heating rate (eq. [3]). The advective rate equals zero when the entropy gradient is zero (at $r \approx 18$ and $r \approx 40$, for $\dot{m} = 10$ and $\dot{m} = 28$, respectively). Outside those radii, advection provides rather small additional cooling in both cases. Inside these radii advection acts as a strong source of heating. (b) Mach number and (c) ratio h/r for the same cases as in panel (a). The styles of the curves are the same as in panel (a).

Table 1. Models

N	$\dot{m}$	$l_{\rm in}$	r_s
1	10	3.570	9.90
2	10	3.782	12.02
3	10	4.025	13.95
4	13	4.010	15.0
5	13	4.170	16.4
6	15	4.125	16.6
7	15	4.513	19.9
8	17	4.251	18.8
9	17	4.850	23.9
10	19	4.416	18.6
11	19	5.088	25.8
12	28	4.305	22.1
13	28	5.169	30.6
14	28	5.409	33.0

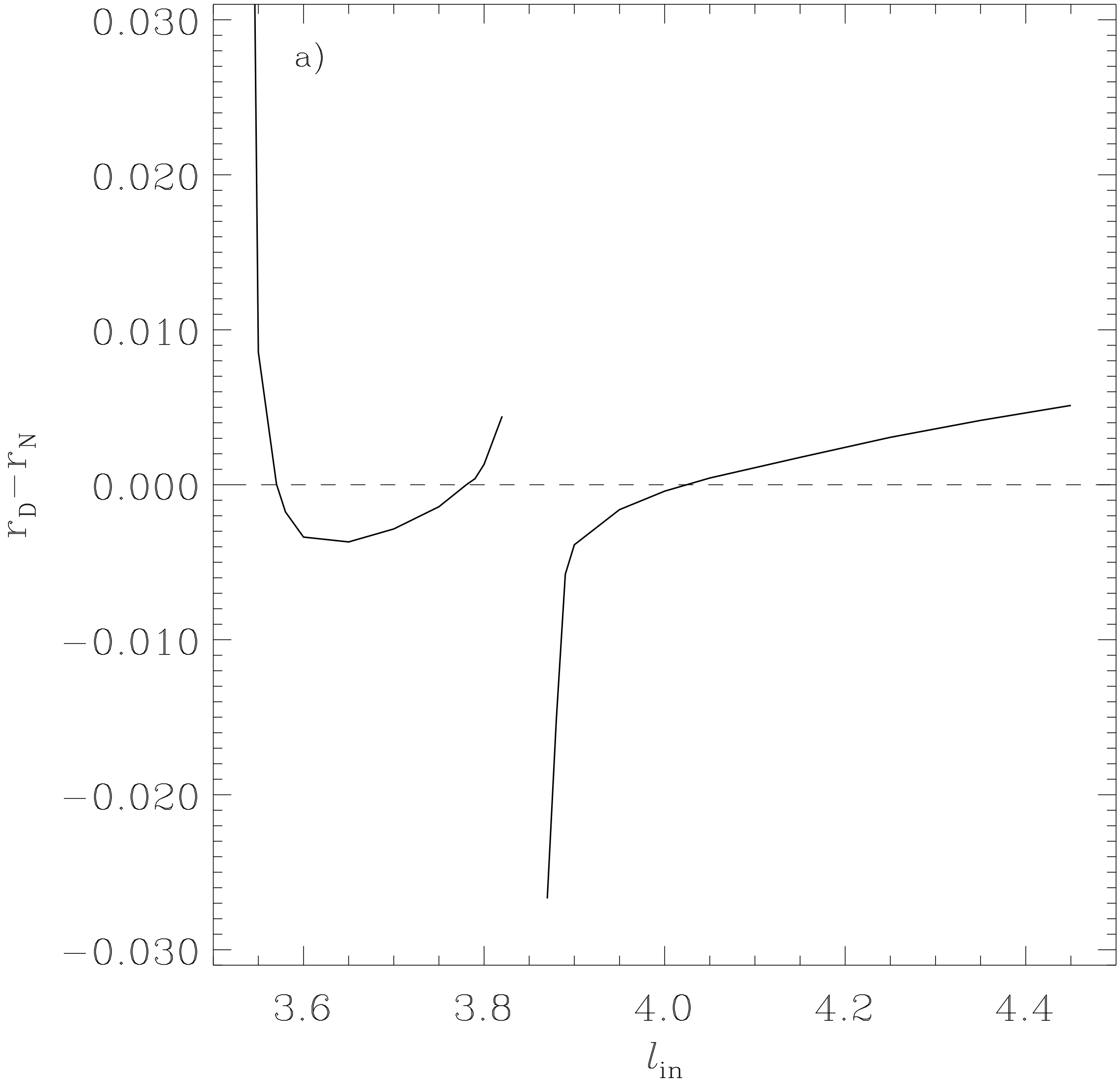

a)
0.030
0.020
0.010
0.000
−0.010
−0.020
−0.030
$r_D - r_N$
3.6
3.8
4.0
4.2
4.4
l_{in}

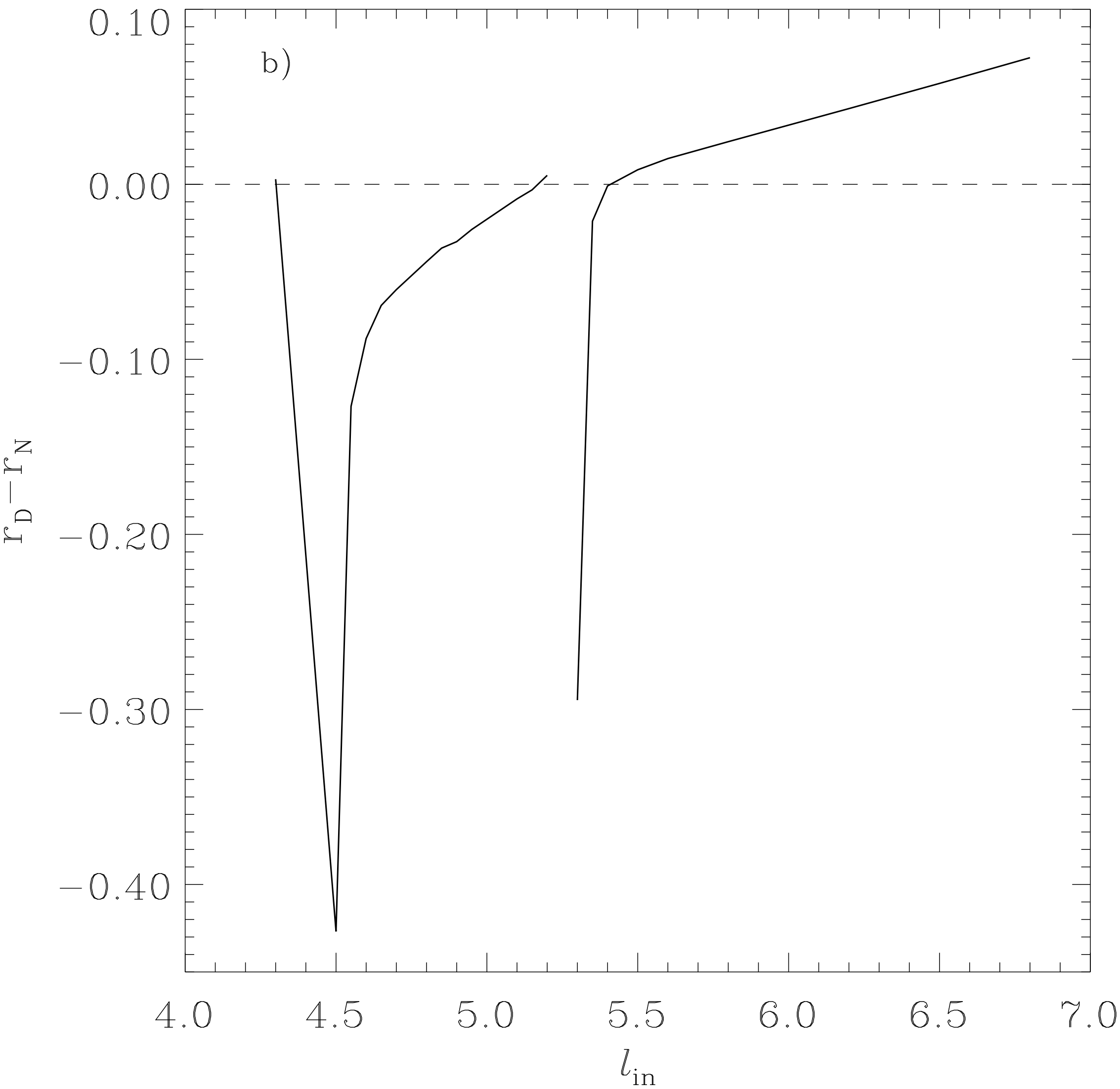

b)
0.10
0.00
−0.10
−0.20
−0.30
−0.40
$r_D - r_N$
4.0
4.5
5.0
5.5
6.0
6.5
7.0
l_{in}

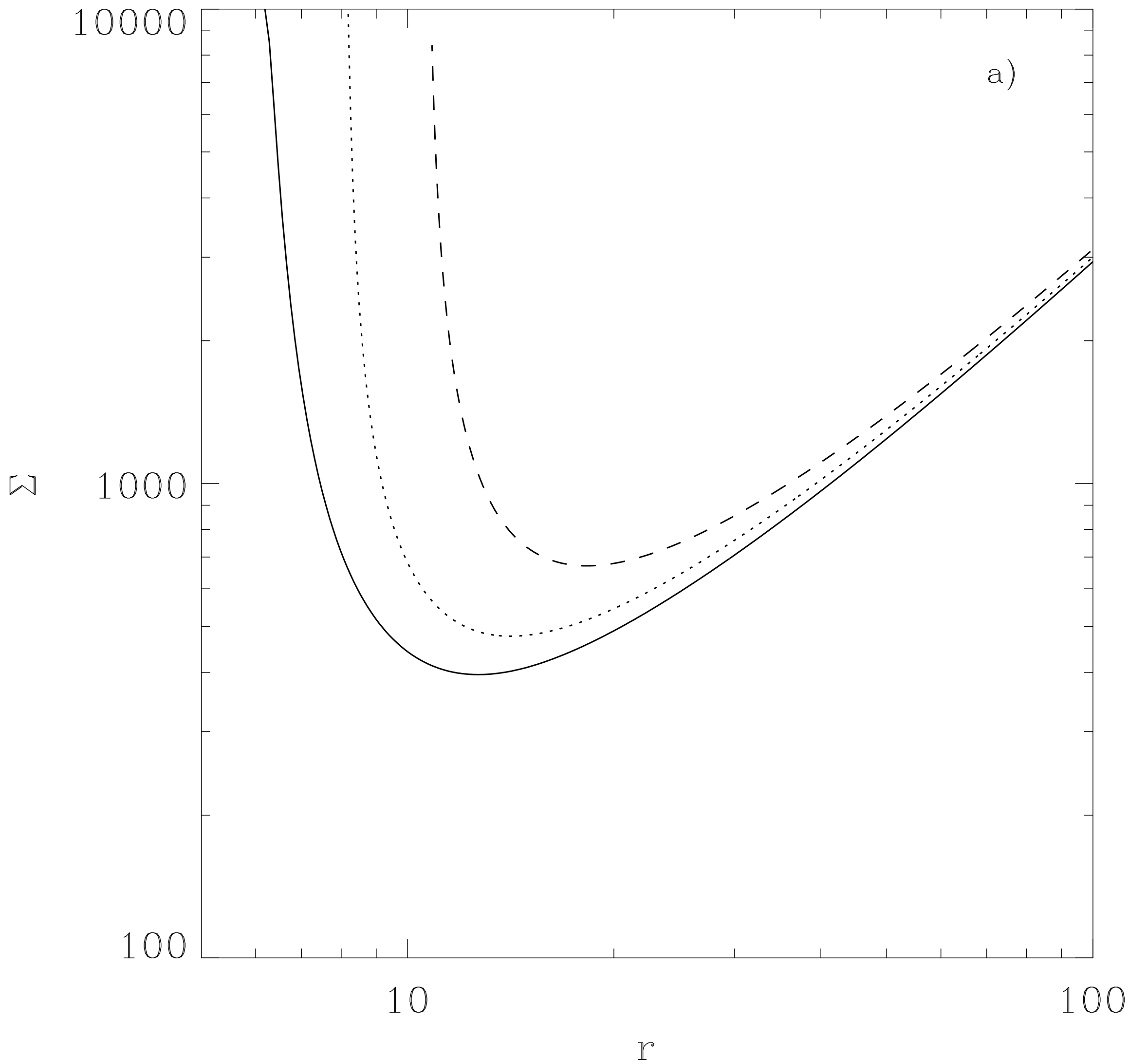
a)
10000
1000
100
Σ
10
100
r

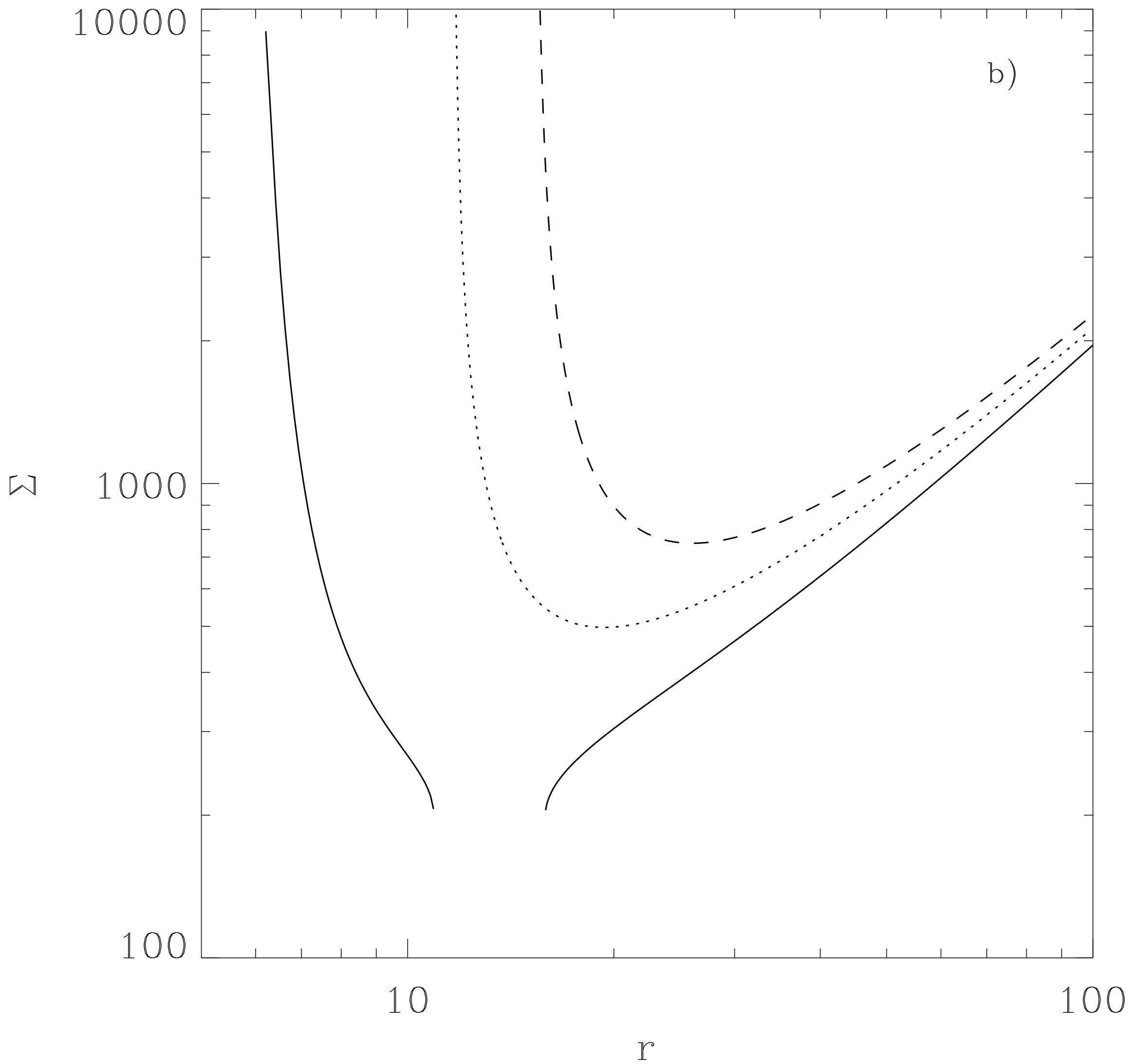

10000
1000
100
10
100
r
Σ
b)

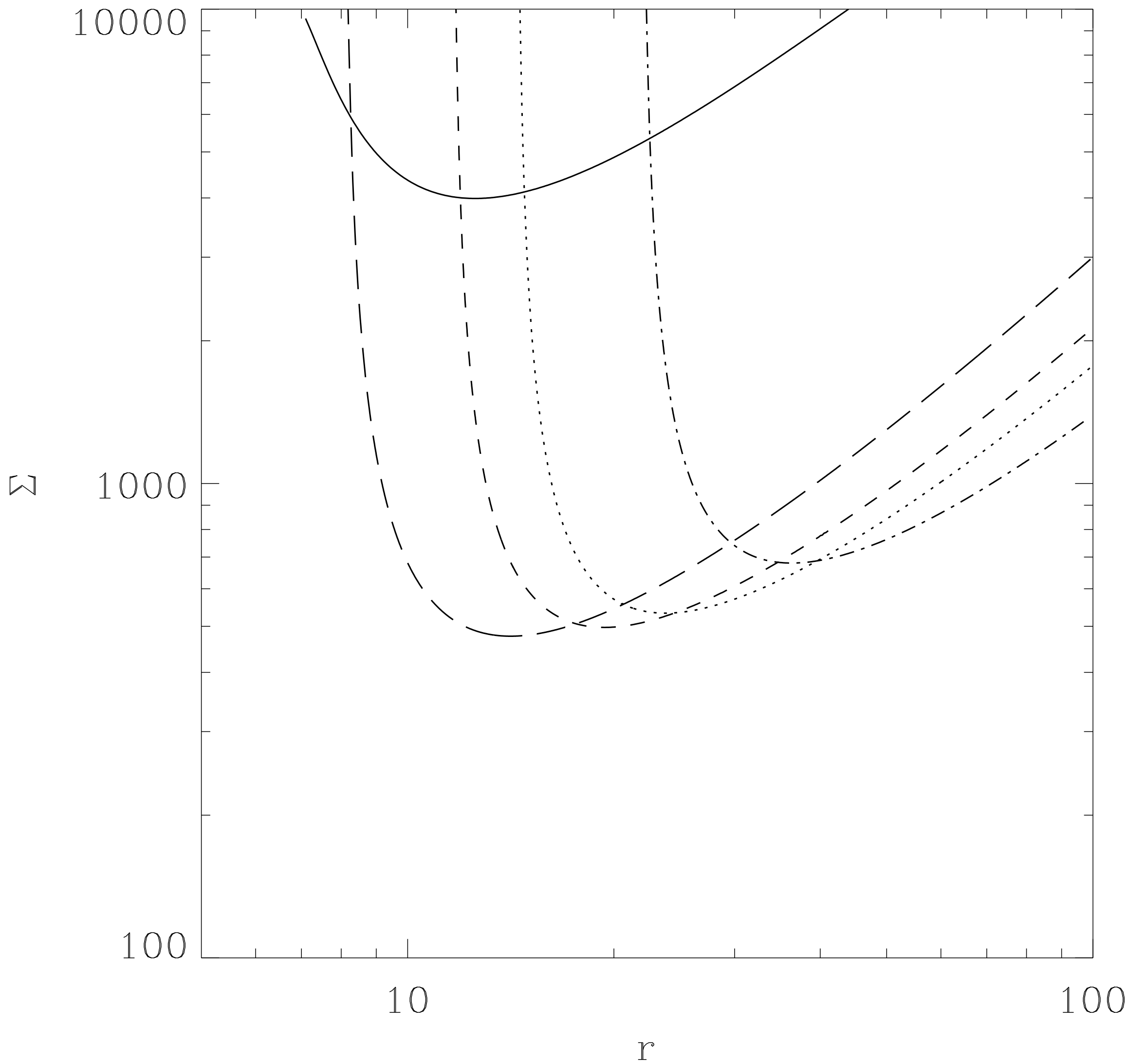
10000
1000
100
10
100
r
Σ

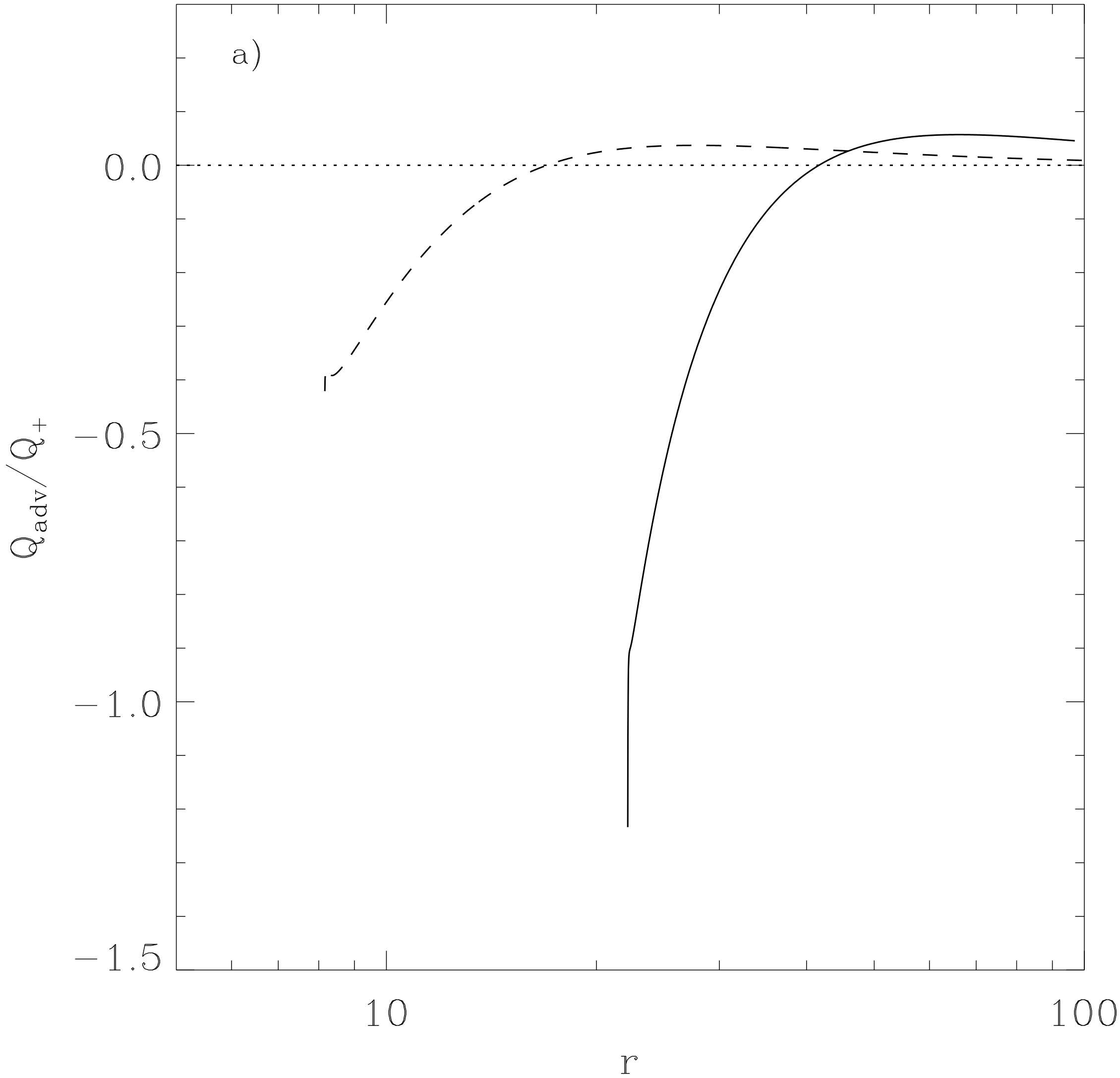

a)
0.0
−0.5
−1.0
−1.5
$Q_{\rm adv}/Q_{+}$
10
100
r

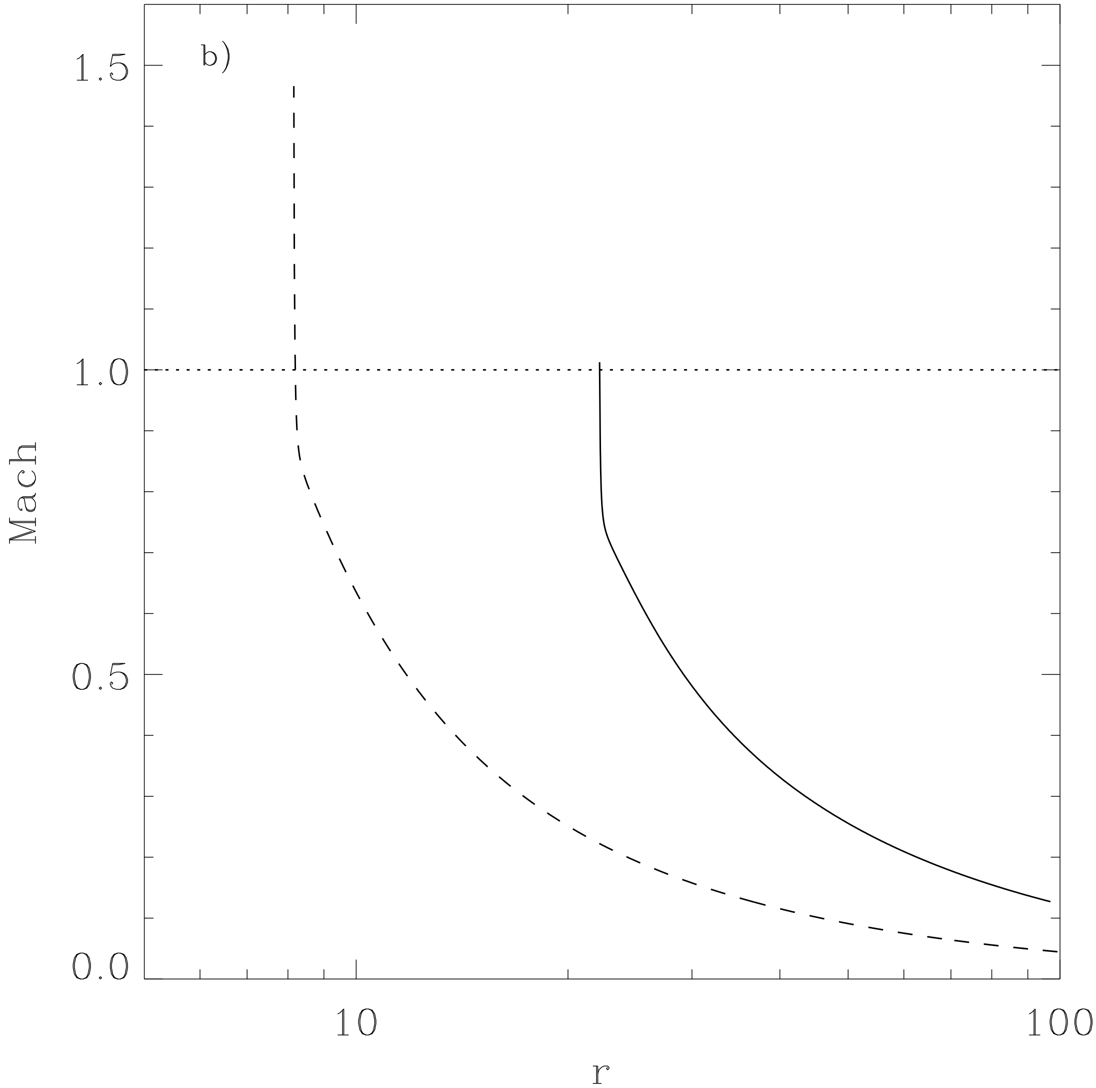
b)
1.5
1.0
0.5
0.0
Mach
10
100
r

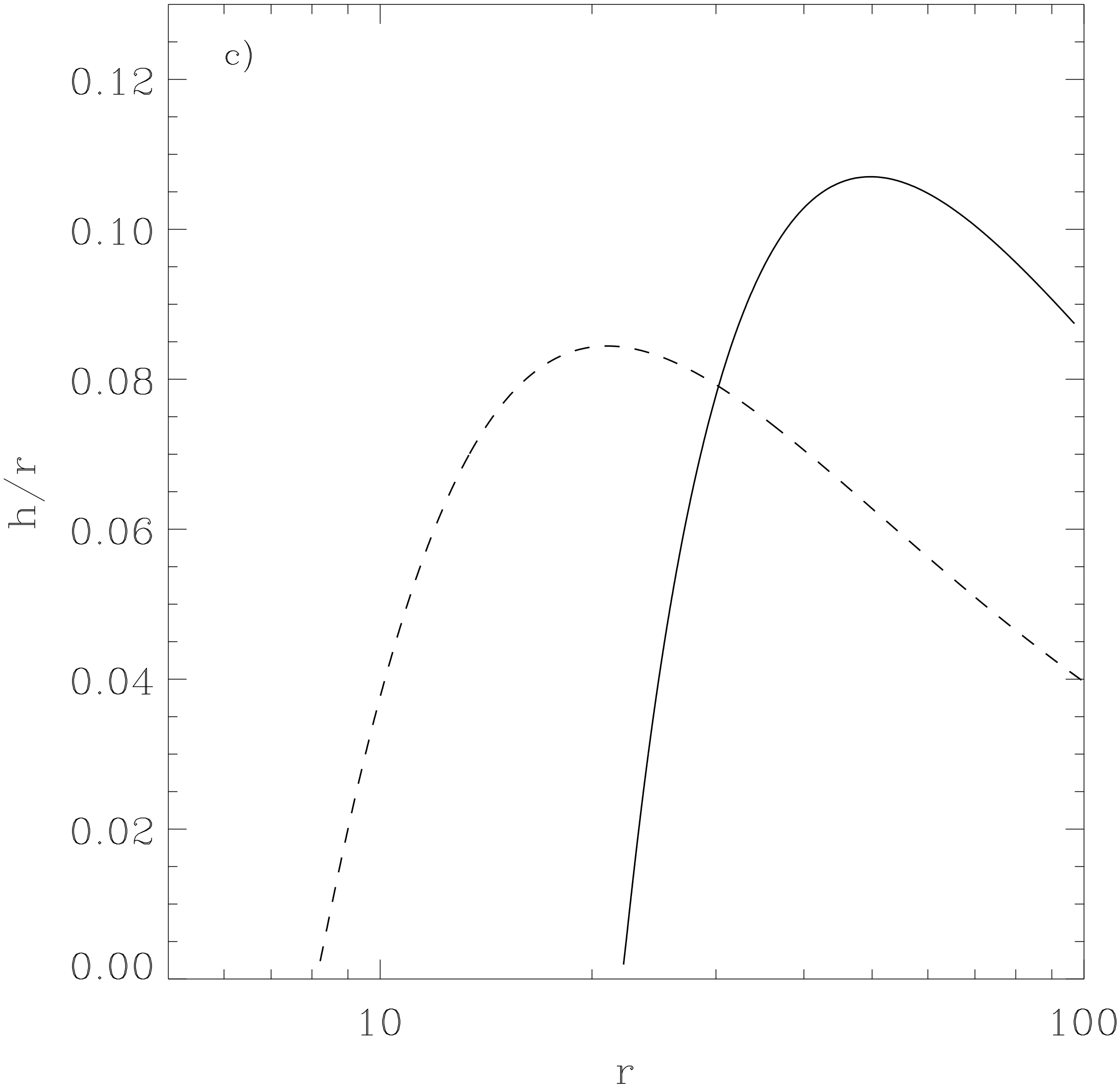

c)
0.12
0.10
0.08
0.06
0.04
0.02
0.00
h/r
10
100
r